Eur. Phys. J. B **13**, 235–243 (2000)

THE EUROPEAN PHYSICAL JOURNAL B

EDP Sciences

Magnetic properties of mixed graphite containing both hexagonal and rhombohedral forms

S. Chehab, K. Guérin, J. Amiell, and S. Flandrois[a]

Centre de Recherche Paul Pascal, CNRS, avenue A. Schweitzer, 33600 Pessac, France

Received 4 February 1999 and Received in final form 28 April 1999

Abstract. Magnetic properties of graphite materials containing variable fractional amounts (up to 40%) of the Rhombohedral graphite form have been investigated by means of electron spin resonance. The variations with temperature and rhombohedral content of the Landé g-factor, ESR linewidth and paramagnetic spin-susceptibility have been analyzed. A narrow parallelism in the behaviours of the g-factor, linewidth and diamagnetic susceptibility (as the latter is known from an earlier work by Gasparoux) has been perceived, conforming to a similar parallelism between these three physical quantities present in earlier works on graphitic-type systems, but there, as a function of high-temperature-treatment and dopant concentration. From the g-value results, the g-anisotropy of the rhombohedral structure is inferred. The paramagnetic spin-susceptibility shows an increased tendency toward 2D character with increased rhombohedral content, in agreement with the theoretical predictions of McClure concerning (hypothetical) rhombohedral graphite.

PACS. 81.05.Tp Fullerenes and related materials; diamond, graphite – 76.30.-v Electron paramagnetic resonance and relaxation – 75.30.Gw Magnetic anisotropy

1 Introduction

The physical properties of graphite as well as graphitic-type systems have been for the last eighty years or so the subject of a very large number of investigations and studies [1–4].

The peculiar properties of graphite in general, and its magnetic behaviour in particular – the topic of this study –, which is characterized by a very large and highly anisotropic diamagnetic susceptibility χ_{d}, are believed to ensue from an interplay between an aromatic (benzene-like) configuration of the carbon atoms at the molecular level, and a layered structure, with a strong two-dimensional (2D) character, at the crystallographic level [4–10]. The inter-graphene-layer interactions (*i.e.* the 3D character), although they are known to be very weak relative to the intra-layer interaction, still play an important role by perturbing the perfect two-dimensionality of the system, in turn, creating a non-zero band-overlap and a finite Fermi surface. It turns out that the shape, volume and energy of the Fermi surface and, consequently, the subtilties of the electronic behaviour are very sensitive to the way the graphene layers are stacked [11–24].

The most common form of graphite, known to exist naturally and synthetically, is called Bernal hexagonal graphite (B-H-Gr) and is characterised by a stacking sequence of the type ABABAB... [25]. Another less common form of graphite, that is also found to occur naturally and synthetically, but never in isolation, is known as rhombohedral graphite (Rh-Gr); the latter is characterized by a stacking sequence of the type ABCABCABC..., and is always obtained in association, mixed with the Bernal type [19,21,26,27]. As a matter of fact, it has been theoretically found, from an *ab initio* study, that the total energy of Rh-Gr is slightly larger, by 0.11 meV/atom, than that of B-H-Gr [21]; this can explain the reason why the rhombohedral phase is only observed to exist in combination with the hexagonal phase and in relatively smaller percentages. As a result, the physical properties and behaviour of rhombohedral graphite could not easily be explored and hence, at least experimentally, are still not well known.

In this work, B-H-Gr samples containing increasing volume-fractions, up to $\sim 40\%$, of the rhombohedral phase are investigated. The magnetic behavior of these graphitic mosaic combinations, and the effects brought about by the presence of the rhombohedral modification are probed with the aid of the electron spin resonance (ESR) technique. The results are analysed and correlated with past experimental and theoretical works.

2 Experimental procedures

Three powder samples of commercial graphite containing approximately 5, 15 and 40% of the rhombohedral phase have been selected. This fractional amount of the rhombohedral content (Rh%) was estimated using X-ray diffraction by comparing the intensities of the (101) peaks of

[a] e-mail: flandrois@crpp.u-bordeaux.fr

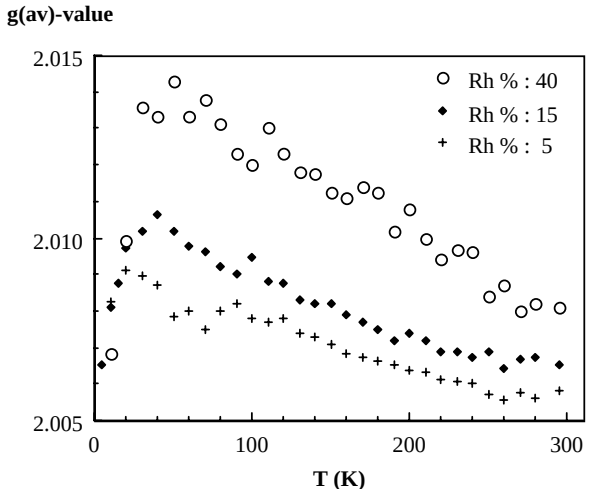

Fig. 1. Variation of the $g_{(\mathrm{average})}$-value with temperature for the three samples having rhombohedral-phase content Rh% = 5, 15 and 40%.

both crystalline forms [18,27,28]. The width of the diffraction peaks were similar for both phases and close to the instrumental broadening, whatever the percentage of rhombohedral phase. The corresponding coherence lengths can be estimated to be several hundred Å.

ESR measurements were performed at the X-band frequency ($\sim$ 9.3 GHz) using a field-modulated spectrometer in the temperature range between 4.2 K and room temperature (RT). Prior to the ESR measurements, the samples were treated with concentrated hydrochloric acid at reflux, in order to remove possibly present ferromagnetic metallic impurities; the samples were, then, thoroughly washed with water until complete elimination of chloride ions, and finally dried. The as-cleaned powder samples were placed into quartz tubes which were subsequently sealed under vacuum. For the ESR measurements, the sealed tubes (with samples) were held vertically, and hence they were in a perpendicular position to the static applied magnetic field (the latter being mainly in the horizontal plane). Consequently, since the platelet-like particles of graphite tended to stack up in layers, as they would naturally do following from their layered crystal structure, the field direction thus tended to be parallel to the crystallites graphene planes. All this led to a configuration in which the crystallites (of our polycrystalline graphite samples) retained an average preferential orientation relative to the magnetic field and for which, given the smallness of the particle size, the skin effect was negligible [29,30].

The observed ESR spectra show a slightly asymmetric single line characteristic of mobile charged-carrier spins in anisotropic graphite particles [29,30]. From these lines, the Landé g-factor, ESR linewidth (ΔH) and paramagnetic spin-susceptibility (χ_{p}) were obtained.

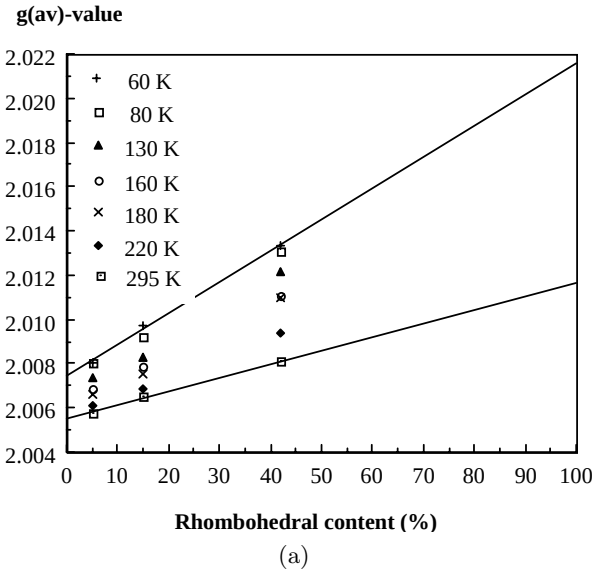

(a)

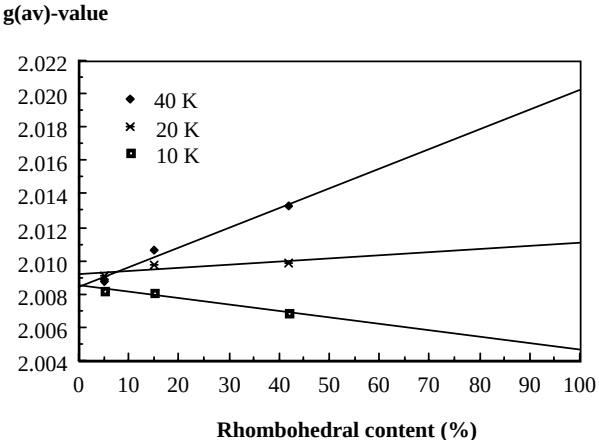

(b)

Fig. 2. Variation of the $g_{(\mathrm{av})}$-value with rhombohedral content for constant temperatures.

3 Results and analysis

3.1 g-factor

It is clear from Figure 1 that the g-factor, as measured from the ESR spectral line, depends on both temperature and Rh%. For a given Rh%, and as T is lowered from room temperature (RT), the g-factor behaviour is characterised by a continuous increase in its value, reaching a maximum (at a temperature we call $T_{M(g)}$) in the lower temperature region; this is followed by a quick decrease in the g-value with continuing falling T. Further, at a given constant temperature (T larger than $\sim$ 20 K), the g-value rises monotonically with increasing Rh%; this is well demonstrated in Figure 2 where a linear relationship can easily be inferred for the g-value *versus* Rh% dependence.

To have more of a quantitative insight into the g-value dependence on temperature, the variation of $\mathrm{Ln}(g)$ against

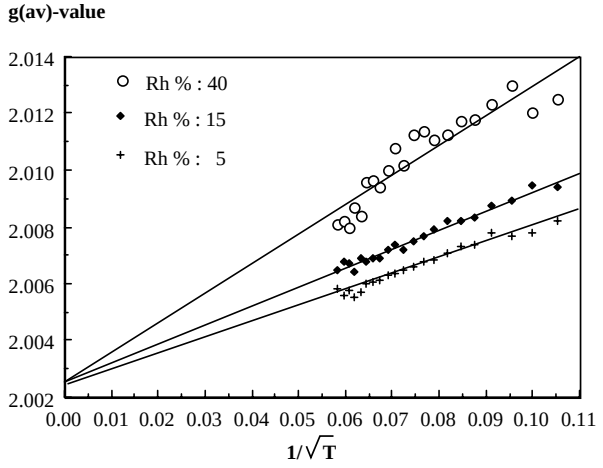

Fig. 3. Linear dependence of the $g_{(\mathrm{av})}$-value plotted as a function of $T^{-0.5}$ in the higher (than ∼100 K) temperature region.

Ln(T) was plotted. This shows a linear dependence for temperatures above 100 K, with a slope of ≈ -0.5. Indeed, plotting the g-value as a function of $1/T^{0.5}$ exhibits a linear behaviour as it is evident in Figure 3 for the three samples with Rh% = 5, 15 and 40%. Furthermore, the extrapolations of the three fitted straight lines converge to the same intercept (at $T = \infty$) of $g_\infty \approx 2.0026$. This is quite significant as it corresponds to the value of $g_\perp$ (obtained when the magnetic field is applied parallel to the graphene layers and hence perpendicular to the c-axis of single crystal graphite) [29–32]. Taking into account the crystallographic in-plane and axial symmetries of graphite, the g-value can have the following general expression [33]:

$$g = [g_\perp + C(\theta)\Delta g] \tag{1a}$$

where $\Delta g = g_\parallel - g_\perp$, known as the g-factor anisotropy, (and $g_\parallel$ corresponds to the magnetic field applied parallel to the c-axis of single crystal graphite and hence perpendicular to the graphene layers). $C(\theta)$ describes the angular variation of the g-factor with θ, the angle between the applied magnetic field direction and the c-axis of the graphitic crystallite. For a single crystal $C(\theta)$ was found to behave like a $\cos^2\theta$ function [31]. In the case of a polycrystalline graphite with its crystallites having a statistical random-Gaussian orientation, the distribution relative to the applied magnetic field direction, $C(\theta)$, takes an average value $C_{\mathrm{av-rand}} = 1/3$, and hence the observed g-value represents, in this case [29,30,33–36], an average value $g_{\mathrm{av-rand}} = [g_\perp + \Delta g/3]$. As for this study, our measured g-value also represents an average value (g_{av}) for polycrystalline graphite, but here, as indicated above, the crystallites have a preferential orientation distribution relative to the applied magnetic field, the direction of which tended to be parallel to the graphene planes. We write:

$$g_{\mathrm{av}} = [g_\perp + C_{\mathrm{av}}\Delta g] \tag{1b}$$

C_{av}, which is directly related to the collective angular average ($\underline{\theta}$) of the crystallite orientations, can be determined as follows: By extrapolating the linear behaviour of the g-value *vs.* Rh% (shown in Fig. 2) to Rh% = 0%, one can estimate the g_{av} values that the pure Bernal-hexagonal phase would have for the various measurement temperatures; and knowing its (B-H-Gr) anisotropy Δg *versus* T [31] as well as $g_\perp = 2.0026$, a mean-value for C_{av} (considered T-independent [18,30,33–36]) can then be calculated and is found to be $\approx 1/25$. Assuming that $C_{\mathrm{av}} = [\underline{\cos\,\theta}]^2$ [30,33–36], we can hence estimate the average angle $\underline{\theta}$ to be roughly around 78°.

Given the fact that $g_\perp$ is always a constant independent of physical variables such as temperature, doping, HTT and others, and that C_{av} can be safely considered to be the same for all our samples independent of T, the variation of g_{av} is thus due solely to the shifting of $g_\parallel$ or, equivalently, of the anisotropy Δg [18,31,33–36]. It follows that our experimental data for the g-factor are well described by equations (1), where an increase in temperature leads to a decrease of the anisotropy ($\Delta g \propto T^{-0.5}$), which eventually goes to zero when T tends to infinity, leaving a g-value equal to $g_\perp = 2.0026$. It is worth noting that Singer and Wagoner's g-value data for polycrystalline graphite [29] have a similar temperature dependence to ours: their data replotted as a function of $1/T^{0.5}$, also, exhibit a linear variation.

One can go further and determine $g_\parallel$ for Rh-graphite: by extrapolating the straight line behaviour in Figure 2 to Rh% = 100%, one can obtain g_{av} for the pure rhombohedral phase; then, assuming the same average orientation for the rhombohedral crystallites (and hence the same C_{av}), and of course the same $g_\perp$ value, $g_\parallel^{(\mathrm{Rh-Gr})}$ can be estimated and is found to be ≈ 2.24 at RT, compared to 2.05 for the hexagonal graphite. Repeating the same procedure for the different measurement temperatures allows us to obtain the variation of $g_\parallel^{(\mathrm{Rh-Gr})}$ with T; the latter is presented in Figure 4. This result and the g-value dependence on Rh% will further be discussed later in connection with the diamagnetic susceptibility.

3.2 Linewidth

With regards to the ESR linewidth (ΔH), it is interesting to note that ΔH appears to exhibit an analogous behaviour to that of the g-factor in connection to its dependence on T and Rh%. This is seen by comparing Figures 5 (ΔH *vs.* T) and 6 (ΔH *vs.* Rh%) to Figures 1 (g-value *vs.* T) and 2 (g-value *vs.* Rh%). Moreover, a closer comparative look at Figures 1 and 5 reveals that the temperatures, $T_{M(g)}$ and $T_{M(\Delta H)}$, at which the maxima occur are very close, and both shift to higher values in the same manner when Rh% is increased. Furthermore, the plotting of ΔH *versus* $1/T^{0.5}$, presented in Figure 7, also reveals a linear behaviour for T >100 K. All this points to a direct correlation between the g_{av}-value and the linewidth. A similar indication was given before by Pacault *et al.* and by Delhaes [34,37], but their observations were made in connection to high-treatment-temperature (HTT for pre- and graphitic carbons) as the major variable. In fact, ΔH

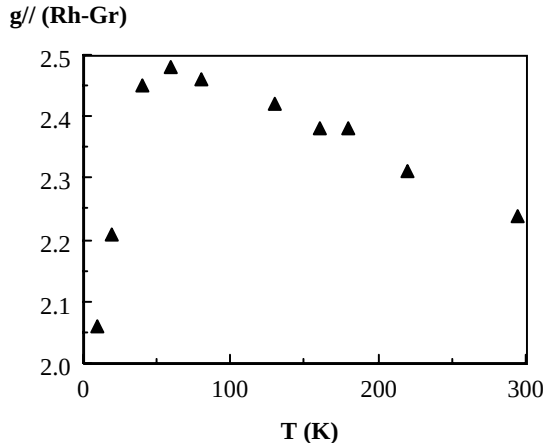

(a)

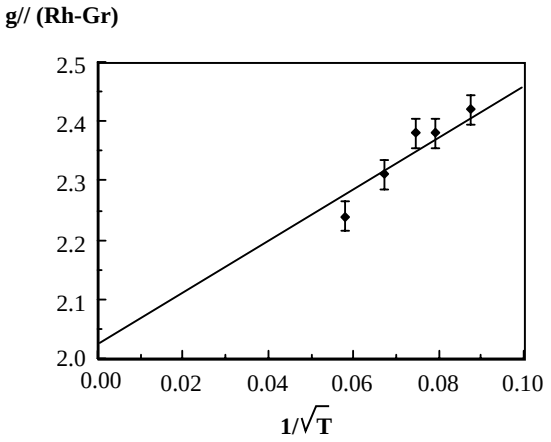

(b)

Fig. 4. Temperature variation of calculated $g_{\|}$-value for rhombohedral graphite (a); the $g_{\|}$-value data plotted as a function of $T^{-0.5}$ in the higher (than $\sim$ 100 K) temperature region (b).

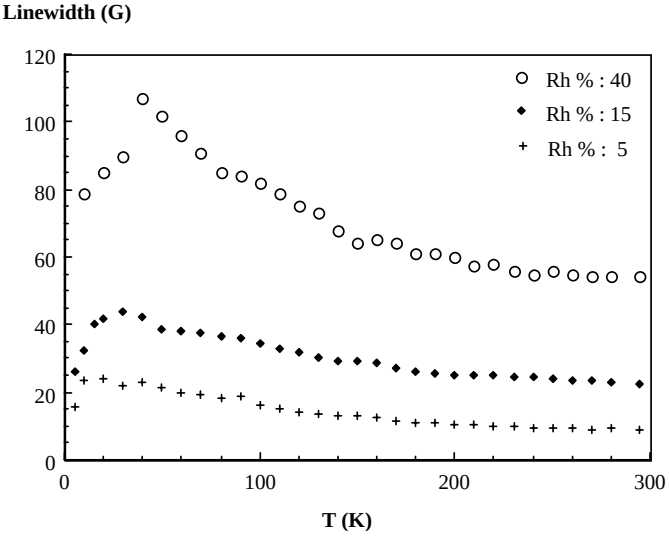

Fig. 5. Variation of the ESR linewidth ΔH with temperature for the three samples having rhombohedral-phase content Rh% = 5, 15 and 40%.

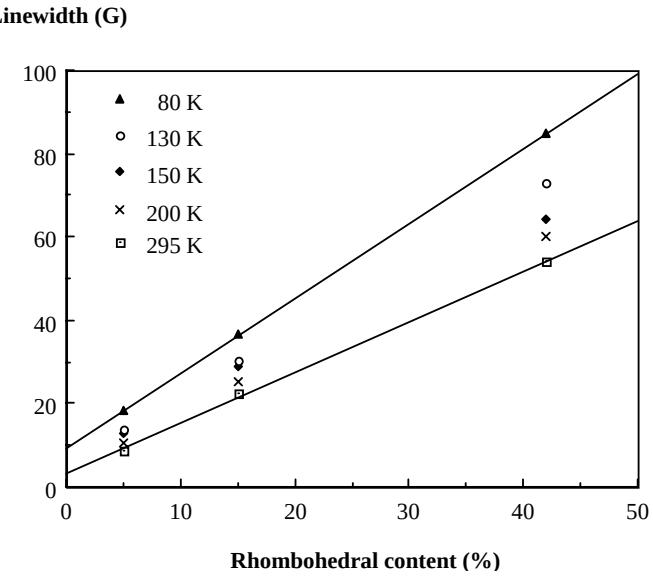

Fig. 6. Variation of the ESR linewidth ΔH with rhombohedral content for constant temperatures.

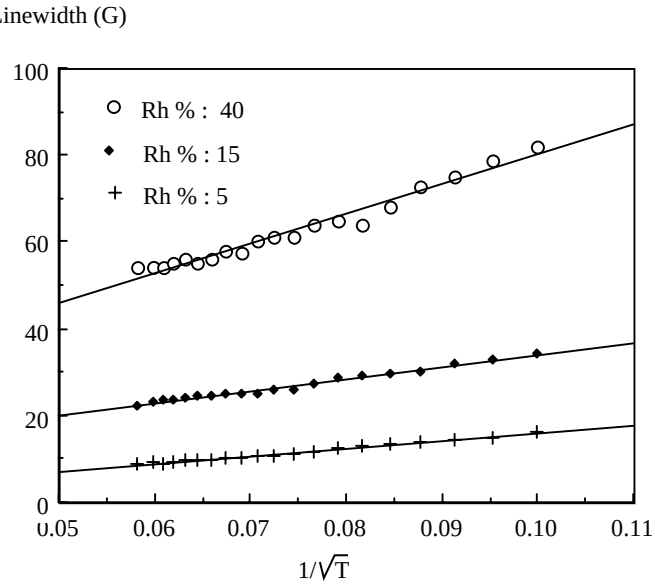

Fig. 7. Linear dependence of the ESR linewidth ΔH plotted as a function of $T^{-0.5}$ in the higher (than $\sim$ 100 K) temperature region.

is thought to be determined primarily by the anisotropy Δg, and hence the observed ESR line represents the collective envelope of the resonance lines resulting from the individual differently-oriented crystallites [29,30,34].

3.3 Comparison with diamagnetic behaviour

It is relevant to compare our study with the earlier and pertinent work of Gasparoux [18], who investigated the diamagnetic susceptibility ($\chi_{\rm dia}$) of polycrystalline graphite samples (also) containing variable fractional amounts (0-22%) of the rhombohedral phase.

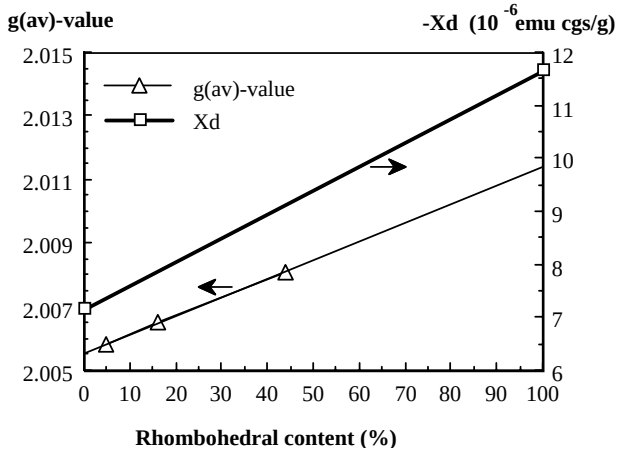

Fig. 8. Average diamagnetic susceptibility $\chi_{\rm dia}$ (Gasparoux [18]) and $g_{\rm (av)}$-value (data at room-temperature) shown together as a function of Rh%, illustrating a parallel in the behaviour of both physical parameters.

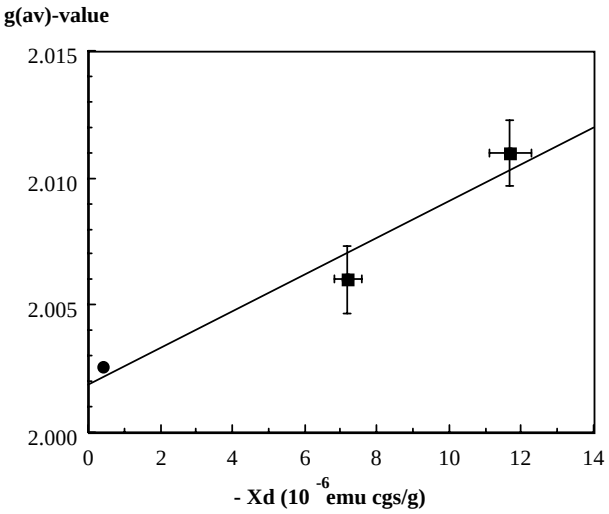

Fig. 9. $g_{\rm (av)}$-value *versus* $\chi_{\rm dia}$; a replot of the data of Figure 8 the linear extrapolation of which heads toward the graphite constant parameters $\{g_\perp, \chi_\perp\}$ (represented by the full circle), demonstrating a universality in the direct relationship between the diamagnetic susceptibility and the g-factor in graphitic systems.

He perceived the existence of a linear proportionality between $\chi_{\rm dia-av(erage)}$ and Rh%, similar to our observation for $g_{\rm av}$ *versus* Rh% (as seen in Fig. 2). One thus can infer that there are parallels between the $\chi_{\rm dia-av}$ and $g_{\rm av}$ behaviours. This is clearly illustrated in Figure 8, where both Gasparoux's data for $\chi_{\rm dia-av}$ and our data for $g_{\rm av}$ are together shown as a function of Rh%; both are linearly increasing functions of Rh%. Note that, similarly, Castle *et al.* [38] and Pacault *et al.* [33,37], in earlier works in which they have studied the effects of HTT on various properties of pre- and graphitic carbons, noted the existence of a correlation between $\chi_{\rm dia}$ and the g-factor; this was reviewed and reiterated later by Marchand [39]. Additionally, a simultaneous and dramatic reduction, of approximately the same order of magnitude, in the $\chi_{\rm dia}$ and g-factor anisotropy is found to occur upon doping graphite (even slightly) with an acceptor, such as boron or bromine, and hence changing (even slightly) its Fermi level [31,32,36,40,41].

In an attempt to give this correlative character (between $\chi_{\rm dia}$ and the g-factor) a more quantitative picture, one can, based on the information gained from Figure 8, directly plot the variation of $\chi_{\rm dia-av}$ *versus* that of $g_{\rm av}$. This is done in Figure 9, where the two illustrative end points corresponding to Rh% = 0 and Rh% = 100 are displayed along with the point of "fixed" coordinates $\{g_\perp, \chi_\perp\}$, which are known to be constant, independent of the variation of various physical quantities [6–8,29–36,40–43]. Within the experimental errors, a straight-line curve can be drawn through these points, pointing to a direct proportionality between the g-factor and the diamagnetic susceptibility for graphitic systems.

4 Discussion

As a matter of fact, according to Fukuyama [44,45], and as reviewed by White [46], both the large diamagnetic susceptibility and the substantial deviation of the g-factor from the free-spin value of $g_{\rm e} = 2.0023$, (both of which) observed in semimetallic systems, such as Bi, and in small-band-gap semiconductors, such as InSb, [47–51], have the same physical origin. The interplay between (i) the perturbing influence of the applied magnetic field (triggering of interband effects), (ii) the smallness of the band-gap (or the band-overlap) and (iii) the lightness of the electronic effective mass (ii and iii are a direct consequence of the electronic band structure), coupled with the facts that (iv) the Fermi level lies in or very close to the band-gap (or the band-overlap) region and that (v) the spin-orbit interaction is of comparable magnitude to or larger than the energy gap, (all these combined) give rise to "enhanced" Landau orbitals. It is these extended electronic orbitals which (a) produce a more effective opposition to the applied magnetic field, leading to a higher than usual $\chi_{\rm dia}$, and (b) admix to the electron-spin intrinsic moment (*via* spin-orbit coupling), resulting in a larger effective magnetic moment and, hence, the g-factor departure from $g_{\rm e}$. There is no question that graphite fulfills those conditions stated above, as it has been shown by Sharma [40] *et al.* and later by Maaroufi *et al.* [41] that the theoretical formulations of Fukuyama explain extremely well the behaviour of graphite's diamagnetic susceptibility. In addition, it should be noted that Levintovich and Kotosonov [8] have, based on the above mentioned physical criteria, derived theoretical expressions for the orbital susceptibility of a "two-dimensional" graphitic system (in which the inter-graphene-layer interactions are considered to be null), which provided a satisfactory description of experimental data obtained earlier for graphitic pyrocarbons.

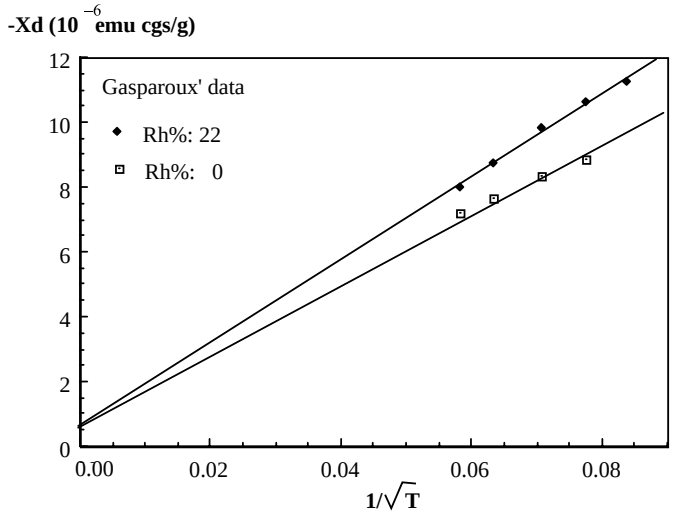

Fig. 10. $\chi_{\rm dia}$ experimental data of Gasparoux [18] replotted here as a function of $T^{-0.5}$ in the higher (than $\sim$ 150 K) temperature region.

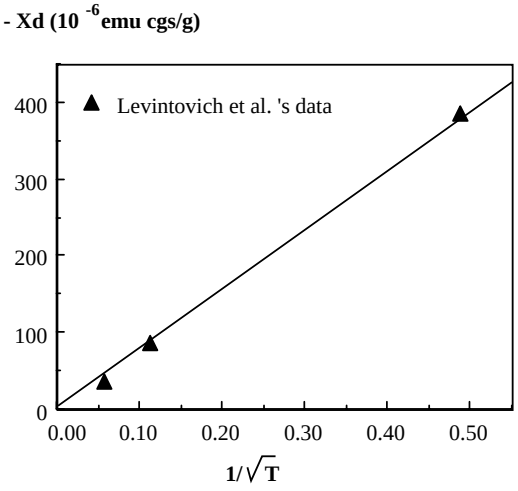

Fig. 11. $\chi_{\rm dia}$ theoretical data of Levintovich and Kotosonov [8] for 2D graphite replotted here as a function of $T^{-0.5}$ for $T = 4.2$, 77 and 300 K.

4.1 Parallelism between diamagnetism and g-factor

We can, based on empirical considerations, elaborate further on the question of the analogous behaviour between $\chi_{\rm dia-av}$ and $g_{\rm av}$ as a function of temperature. We show in Figure 10 that Gasparoux's data [18] of $\chi_{\rm dia-av}$ *versus* T have, for $T > 150$ K or so, the same temperature variation as our $g_{\rm av}$ data, *i.e.* a $1/T^{0.5}$ dependence. As can be seen also, the linear curves in Figure 10, for the different Rh%, extrapolate toward the constant $\chi_\perp$ value of $\approx -0.5 \times 10^{-6}$ emu/g, when T goes to infinity. This is in complete concordance with the behaviour of $g_{\rm av}$ in Figure 3, which extrapolates to $g_\perp$, as discussed earlier. Furthermore, Levintovich and Kotosonov [8], in the work mentioned above, have theoretically calculated values for $\chi_\parallel$, at $T = 4.2$ K, 77 K and 300 K, for perfect/ideal "two-dimensional" graphite. The plot of these $\chi_\parallel$ values *versus* $1/T^{0.5}$, presented in Figure 11, shows a straight-line behaviour which extrapolates through the origin; *i.e.* $\chi_\parallel$ vanishes when T goes to infinity, which is plausible. The outcome of this analysis (Fig. 11) seems to carry quite an interesting physical significance. It appears that the $1/T^{0.5}$ dependence is a characteristic of two-dimensional (2D) behaviour in graphite. The 2D character is enhanced: (i) by raising the temperature, because then the 3D inter-layer interactions are weakened and the graphene planes become more and more independent, and/or (ii) by increasing the degree of stacking disorder of the graphitic layers, because then the correlation between the interaction between successive atomic plane-layers is diminished. The latter situation is believed to take place when going from the highly ordered and hypothetical simple-hexagonal graphite with stacking sequence AAAA..., to the B-H-Gr (stacking sequence ABAB...), to the Rh-Gr (stacking sequence ABCABC...), and, finally, to the most disordered graphite form, known as turbostratic graphite, having random stacking of its graphene layers [17,19–22,52].

With these conceptions in mind, the following observations can be readily understood: (a) the fact that $1/T^{0.5}$ behaviour is effective in the higher temperature region above 100 K, and (b) the fact that $\chi_{\rm dia}$ and the g-factor (which are shown to be closely linked) increase with higher Rh%. As it turns out from experimental observations and theoretical considerations, in graphitic systems, (for a given temperature) enhancing the 2D character results in an increase of the conduction-electron orbital diamagnetism [8,18,20,21,40,43]. This is quite reasonable, since an enhancement of the two-dimensionality corresponds to a reduction in the inter-layer interactions (characterized by the energy band parameters $\gamma_1, \gamma_2, \ldots \gamma_i \ldots$); this in turn leads to a smaller basal effective mass (as the latter is directly proportional to γ_1), hence giving rise to more energetic Landau orbitals [9,15,33,40,53–56].

The remaining point to discuss on this subject concerns the maximum (at $T = T_{\rm M}$), and hence the subsequent decrease (for T lower than $T_{\rm M}$) observed in the $g_{\rm av}$ *versus* T (and concomitantly in the ΔH *versus* T) variation. Two disparate effects/factors are invoked as causing, or contributing to, this behaviour: (a) the narrow parallelism that exists between the g-factor and $\chi_{\rm dia}$ behaviours, and which we have discussed above at some length; (b) the increasing influence, as T gets lower and lower, of localized electronic spins, the latter believed to result from defects/imperfections present in our graphitic systems.

Concerning point (a), McClure *et al.* [7,40] have predicted theoretically, for B-H-Gr the existence of a maximum in the $\chi_{\rm dia}$ *versus* T behaviour at a low temperature of $\sim$ 20-30 K; later, this has been confirmed experimentally by Maaroufi *et al.* [41]. According to Levintovich and Kotosonov [8], from a physical stand-point, the position of the diamagnetism maximum in a graphitic system corresponds to the temperature ($T_{\rm M}$) at which "the relative fraction of the states with the maximum value of the susceptibility is maximal". Furthermore, McClure,

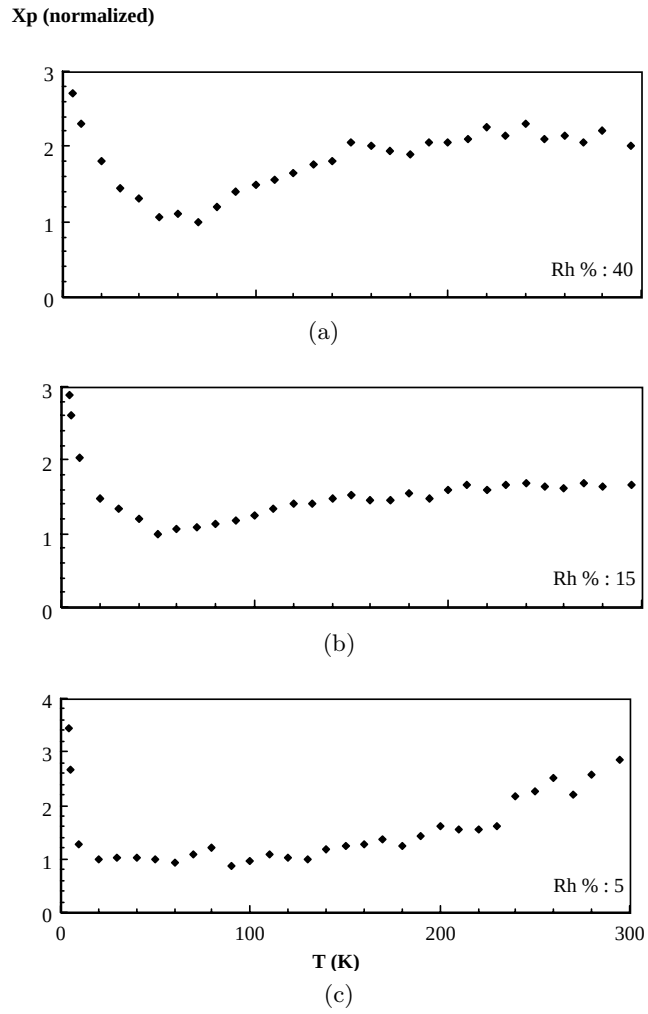

Fig. 12. Temperature dependence of the spin susceptibility (normalized) of the three samples with Rh% = 5, 15 and 40%.

in his theoretical analysis of the electronic properties of Rh-Gr [20], also predicted the existence of a maximum in the diamagnetism of the latter system, at a temperature of $\sim$ 40-50 K (which is clearly higher than that of B-H-Gr). However, to the best of our knowledge, no direct experimental confirmation of this is yet available. Nevertheless, given the direct relationship that exists between $\chi_{\rm dia}$ and the g-factor, the maximum observed in each of our $g_{\rm av}$ *versus* T sets of data, as well as in the deduced $g_{\parallel}$(Rh-Gr) *versus* T behaviour, and the shift of the position ($T_{\rm M}$) of this maximum toward higher temperatures with increasing Rh%, may represent indirect experimental evidence for McClure's theoretical predictions concerning the maximum diamagnetism in Rh-Gr.

As for factor (b), the presence and effect of localized spin centers can be inferred from the low-temperature Pauli paramagnetic susceptibility ($\chi_{\rm P}$) behaviour (see Fig. 12, the full details of $\chi_{\rm P}$ variation will be discussed below) which clearly exhibits a $1/T$ Curie-like dependence. This $1/T$ Curie-like increase ($\chi_{\rm P-loc}$) in $\chi_{\rm P}$ with falling T is additively superimposed above the relatively constant conduction charge-carriers susceptibility ($\chi_{\rm P-cond}$), so that the total $\chi_{\rm P}$ is given by $\chi_{\rm P} = \chi_{\rm P-cond} + \chi_{\rm P-loc}$. Further, a close comparative look at Figure 12 and Figure(s) 1 (and 5) reveals a close correspondence between the onset temperature of the observed Curie-like increase and the temperature of the maximum g-value (and ΔH) $T_{\rm M}$. According to Mrozowski [57], a strong exchange interaction takes place, in such situations, between the free and the localized spin centers, leading to a single ESR line produced with a g-value intermediate between that for the localized spin centres ($g_{\rm loc} \sim g_{\rm free} = 2.0023$) and for the conduction charge-carriers ($g_{\rm cond} = g_{\rm defect-free\ graphite}$). In other words, there will be a simple mixing of the g-values for the two kinds of spin centers; the observed (resultant-average) g-value is weighed by the relative strength of these two types of spins paramagnetic contributions and hence it can be given by the simple mixture formula:

$$g_{\rm av}\chi_{\rm P} = g_{\rm cond}\chi_{\rm P-cond} + g_{\rm free}\chi_{\rm P-loc}.$$

Consequently, in the low temperature region, since $\chi_{\rm P-loc}$ increases as $1/T$, and since $\chi_{\rm P-cond}$ is relatively T-independent, $g_{\rm av}$ will be weighed down toward the $g_{\rm free}$ value. One should add that relatively poor precision at low T made it difficult to obtain an accurate quantitative evaluation of $g_{\rm cond}$.

4.2 Pauli paramagnetism

Moving to the details of the paramagnetic spin-susceptibility ($\chi_{\rm P}$) results presented in Figure 12, these were obtained from the areas circumscribed by the ESR absorption curves. Due to uncertainty about the mass of the samples and to the usual error associated with the spectral-curve integration process, the absolute magnitude of $\chi_{\rm P}$ is not very accurate; however in our analysis, we can safely rely on the relative magnitude of $\chi_{\rm P}$ and its variation with T which are certain. The variation of $\chi_{\rm P}$ with temperature appears to depend on the rhombohedral-phase content. The sample with highest Rh%, $\sim$ 40%, displays the most variability in its $\chi_{\rm P}$ *vs.* T behaviour features; as T is raised from the lowest measurement temperature of 4.2 K, $\chi_{\rm P}$ decreases rapidly to go through a relatively broad minimum, then slowly increases toward a very broad maximum, which looks like a leveling-off region, before showing a tendency to decrease around 250 K. The sample with Rh% $\approx$ 15% shows a similar $\chi_{\rm P}$ *vs.* T behaviour, as described before, except that now T around 250 K concurs with a leveling-off region, and the decreasing tendency of $\chi_{\rm P}$ is believed to take place somewhere above but close to RT, which is beyond the present range of our measurements. As for the sample with the lowest Rh% of $\sim$ 5%, the broad minimum which directly follows the steep decrease of $\chi_{\rm P}$ above 4.2 K appears rather as a wide low plateau spanning over $\sim$ 100 K, in this case, beyond which all we can see is the rise in $\chi_{\rm P}$ up to RT. A careful examination of Wagoner's $\chi_{\rm P}$ data [29] obtained in the temperature range between 100 K and 500 K for B-H-Gr, shows a slow but net increase in $\chi_{\rm P}$, as T is raised from

100 K to around 400 K; beyond the latter temperature χ_P displays a slight but clear decrease, resulting, overall, in a very wide and low maximum centered around 400 K.

The variety of features observed in the χ_P *vs.* T dependence is believed to result from the competing effects of three disparate factors, each one of which would dominate the behaviour of χ_P within a different range of temperatures. These factors are believed to be: (a) the concentration of localized spin-moments resulting from impurities/defects within the graphite system; (b) the magnitude of the degeneracy Fermi temperature, T_F; and (c) the relative strength of the two-dimensional character. Starting from the lowest T (4.2 K) and up to a certain temperature, the value of which depends on Rh%, the effect of the localized spin-moments dominates, as is evident from the $1/T$-Curie-like dependence (the steep decrease) of χ_P. This Curie paramagnetism is then superseded by Pauli paramagnetism, with χ_P exhibiting a levelling-off and/or a relatively slow increase in its magnitude [58]. This behaviour is assumed to be directly related to the relative value of T_F, or more specifically to a factor of the general form $\{1 \pm [T/T_F]^2\}$ [9,59]. As long as T is much smaller than T_F, the squared ratio $[T/T_F]^2$ can be ignored (relative to one) and hence the Pauli susceptibility will exhibit a temperature-independent behaviour; however, when T becomes of the same order of magnitude as T_F, and higher, χ_P is expected then to display a T^2-like variation with temperature. According to Kriessman and Callen [60], the sign of the coefficient of the T^2 term will be positive, *i.e.* the Pauli susceptibility will increase with increasing temperature, if/when the Fermi energy is in the vicinity of a density-of-states minimum. This is, indeed, the case for all allotropic forms of graphite [15,21,52]. Nonetheless, the T_F-value depends on the graphite form considered; in the B-H-Gr case T_F is of the order of 200 K, whereas in Rh-Gr case T_F is lower and of the order of 100 K [18]. Following the reasoning presented above, this difference in the T_F-value may well, therefore, account for the observation that the temperature at which χ_P begins its rise gets smaller with higher Rh%. As the temperature continues to increase, the 2D character becomes more and more influential and the conduction electrons are expected to behave more and more like a two-dimensional Fermi gas, which can lead to the observed decrease in χ_P, as generally expected of the Pauli susceptibility of a 2D Fermi gas with rising temperature [10,34,58]. In the case of pure B-H-Gr [29], χ_P starts its descent above ∼400 K, whereas χ_P for the sample with Rh% = 40% starts going down at ∼250 K. As it appears, increasing the rhombohedral-phase content results in lowering the temperature at which χ_P starts to go down. This is very much in line with our earlier discussions referring to the enhancement of the 2D character in graphitic systems when going from the hexagonal to the rhombohedral structure. In this context, McClure has pointed out that [20], above approximately 150 K, rhombohedral graphite would behave almost like two-dimensional graphite.

5 Conclusion

The magnetic behaviour of mixed graphitic systems, consisting of different combinational proportions of the Bernal-Hexagonal and Rhombohedral forms of graphite, has been the focus of this work. Present electron spin resonance (ESR) measurement results, when considered in conjunction with previously published data, have allowed us to perceive a narrow parallelism in the behaviours of the Landé g-factor, ESR linewidth (ΔH) and diamagnetic susceptibility (χ_{dia}) with varying temperature (T) and rhombohedral content (Rh%). Concerning the T-dependence, all three parameters (g-factor, ΔH and χ_{dia}) dependence in the higher temperature region. It is important to note that a theoretical basis for this empirically observed T-dependence can be found from McClure's theoretical analysis of the rhombohedral graphite electronic properties [20]; there, the calculated χ_{dia} *vs.* T curve, which shows a reasonable agreement with Gasparoux's experimental results [18], indeed varies as $1/T^{0.5}$. As for the variation with Rh%, both the g-value and ΔH increase linearly with increasing Rh%, in analogy to the χ_{dia} *vs.* Rh% linear variation observed by Gasparoux. A direct linear relationship between the g-factor and χ_{dia} has been deduced and presented, and which seemingly extrapolates toward the point of coordinates $\{g_\perp,\ \chi_\perp\}$, the graphite invariable parameters. The extrapolation of the [g-value *vs.* Rh%]$_T$ linear curves allowed us to estimate $g_\parallel^{(Rh-Gr)}$, and hence the g-factor anisotropy for the Rh-Gr phase, and its variation with temperature.

The T- and Rh%-dependence of the paramagnetic susceptibility (χ_p) behaviour indicates, aside from the usual Pauli free-electron spins, also the existence of defect-originating localized spin centers, characterized by a $1/T$ Curie-like behaviour, becoming more and more effective at lower T and for higher Rh%. χ_p shows, as well, in the higher T region, an increased tendency toward 2D character with increased Rh%, in agreement with the theoretical predictions of McClure concerning Rhombohedral graphite [20].

Finally, in order to have further insight into the magnetic properties of these mixed graphitic systems, and by extrapolating into those of the Rh-Gr structure, magnetic susceptometry experiments over the whole temperature range between 4.2 K and RT and for variable magnetic field strengths are being undertaken; the results of these measurements will be presented in a forthcoming paper.

References

1. B.T. Kelly, in *Physics of Graphite* (Applied Science Publishers, 1981).
2. N.B. Brandt, S.M. Shudanov, YaG. Ponomarev, in *Semimetals, Graphite and its compounds*, Modern Problems in Condensed Matter Sciences, Vol. 20.1 (North-Holland, Amsterdam 1988).
3. J.W. McClure, in *Physics of Semimetals and Narrow Bandgap Semiconductors*, edited by D.L. Carter, R.T. Bite (Pergamon, New York, 1971).

4. I.L. Spain, in *Chemistry and Physics of Carbon*, edited by P.L. Walker, P.A. Thrower (Marcel Dekker, NY, 1973 and 1980), Vols. 8 and 15.
5. C.A. Klein, J. Appl. Phys. **35**, 2947 (1964); J. Appl. Phys. **33**, 3338 (1962).
6. J.W. McClure, Phys. Rev. **104**, 666 (1956).
7. J.W. McClure, Phys. Rev. **119**, 606 (1960).
8. I.Y. Levintovich, A.S. Kotosonov, Sov. Phys. JETP **51**, 959 (1980).
9. D.H. Martin, *Magnetism in Solids* (London Illife Books Ltd., 1967), chapter 3.
10. A. Pacault, A. Marchand, in *Proceedings of the Third Conference on Carbon, Buffalo, 1957* (Pergamon Press, 1959), p. 37.
11. J.W. McClure, Phys. Rev. **108**, 612 (1957).
12. J.C. Slonczewski, P.R. Weiss, Phys. Rev. **109**, 272 (1958).
13. P. Nozières, Phys. Rev. **109**, 1510 (1958).
14. J.W. McClure, in *Proc 4th Conf. Carbon* (Pergamon Press, 1960), p. 177.
15. R.C. Tartar, S. Rabi, Phys. Rev. B **25**, 4126 (1982).
16. C.P. Mallett J. Phys. C **14**, L213 (1981).
17. J-C Charlier, X. Gonze, J-P. Michenaud, Phys. Rev. B **43**, 4579 (1991); J-C Charlier J-P. Michenaud, Phys. Rev. B **46**, 4531 (1992).
18. H. Gasparoux, Carbon **5**, 441 (1967).
19. R.R. Haering, Can. J. Phys. **36**, 352 (1958).
20. J.W. McClure, Carbon **7**, 425 (1969).
21. J.-C. Charlier, X. Gonze, J.-P. Michenaud, Carbon **32**, 289 (1994).
22. V. Bayot, L. Piraux, J-P. Michenaud, J-P. Issi, M. Lelaurain, A. Moore, Phys. Rev. B **41**, 11770 (1990).
23. S.J. Williamson, S. Foner, M.S. Dresselhaus, Phys. Rev. **140**, A1429 (1965).
24. D.E. Soule, J.W. McClure, L.B. Smith, Phys. Rev. **134**, A453. (1964).
25. J.D. Bernal, Proc. R. Soc. London, Ser. A **160**, 749 (1924).
26. H. Lipson, A.R. Stokes, Proc. R. Soc. London, Ser. A **181**, 101 (1942).
27. E.J. Friese, A. Kelly, Philos. Mag. **8**, 1519 (1963).
28. R. Gay, H. Gasparoux, in *Les Carbones*, edited by "Groupe Francais d'Étude des Carbones" (Masson, Paris, 1965), p. 63.
29. L.S. Singer, G. Wagoner, in *Proc 5th Conf. Carbon, Penn State* (Pergamon Press, 1961), Vol. 2, p. 65; J. Chem. Phys. **37**, 1812 (1962).
30. P. Delhaes, Carbon **6**, 925 (1968); P. Delhaes, A. Marchand, Carbon **6**, 257 (1968).
31. G. Wagoner, Phys. Rev. **118**, 647 (1960).
32. J.W. McClure, Y. Yafet, in *Proc 5th Conf. Carbon, Penn State* (Pergamon Press, 1961), Vol. 2, p. 22.
33. A. Pacault, J. Uebersfeld, J.G. Theobald, M. Cerrutti, C.R. Acad. Sci. Paris B **261**, 3589 (1965).
34. P. Delhaes, Ph. D. thesis (Doctorat d'État), University of Bordeaux, France, 1965; thesis (3^{e} cycle), University of Bordeaux, France, 1963.
35. E. Poquet, J. Chim. Phys. **60**, 566 (1963).
36. H. Gasparoux, A. Pacault, E. Poquet, Carbon **3**, 65 (1965).
37. A. Pacault, A. Marchand *et al.*, J. Chim. Phys. **57**, 892 (1960).
38. J.G. Castle Jr, D.C. Wobschall, in *Proceedings of the Third Conference on Carbon, Buffalo, 1957* (Pergamon Press, 1959), p. 129.
39. A. Marchand, in *Nouveau Traité de Chimie Minérale*, edited by P. Pascal (Masson et Cie, 1968), p. 497.
40. M.P. Sharma, L.G. Johnson, J.W. McClure, Phys. Rev. B **9**, 2467 (1974).
41. A. Maaroufi, S. Flandrois, C. Coulon, J.C. Rouillon, J. Phys. Chem. Solids **41**, 1103 (1982).
42. J. Heremans, C.H. Olk, T.D. Morelli, Phys. Rev. B **49**, 15122 (1994).
43. D.B. Fischbach, Phys. Rev. **123**, 1613 (1961).
44. H. Fukuyama, R. Kubo, J. Phys. Soc. Jap. **28**, 570 (1970).
45. H. Fukuyama, Prog. Theor. Phys **45**, 704 (1971).
46. R.M. White, *Quantum Theory of Magnetism*, Vol. 46 of Springer Series in Solid-State Sciences (Springer-Verlag, 1983), pp. 68, 82.
47. M.H. Cohen, E.I. Blount, Philos. Mag. **5**, 115 (1960).
48. J.E. Smith, J.K. Galt, F.R. Merritt, Phys. Rev. Lett. **4**, 276 (1960).
49. W.R. Datars, Phys Rev. **126**, 975 (1962).
50. E.N. Adams, Phys. Rev. **59**, 633 (1953).
51. R. Bowers, Y. Yafet, Phys Rev. **115**, 1165 (1960).
52. J-C Charlier, J-P. Michenaud, Ph. Lambin, Phys. Rev. B **46**, 4540 (1992).
53. V.V. Kechin, Sov. Phys. Solid State **11**, 1448 (1970).
54. R.O. Dillon, I.L. Spain, J.A. Woollam, W.H. Lower J. Phys. Chem. Solids **391**, 907 (1978).
55. R.O. Dillon, I.L. Spain, J. W. McClure, J. Phys. Chem. Solids **381**, 635 (1977).
56. E. Mendez, A. Misu, M.S. Dresselhaus, Phys. Rev. B **21**, 827 (1980); A. Misu, E. Mendez, M.S. Dresselhaus, J. Phys. Soc. Jap. **47**, 199 (1979).
57. S. Mrozowski, Carbon **3**, 305 (1965).
58. P. Delhaes, A. Marchand, J. Phys. France **28**, 67 (1967); C.R. Acad. Sci. Paris B **256**, 3296 (1963).
59. D.E.G. Williams, *The Magnetic Properties of Matter* (Longmans, 1966), chapter 3.
60. C.J. Kriessman, H.B. Callen, Phys. Rev. **94**, 837 (1954).